New Journal of Physics
The open-access journal for physics

Experiments on wave turbulence: the evolution and growth of second sound acoustic turbulence in superfluid ^{4}He confirm self-similarity

A N Ganshin[1,2], V B Efimov[1,3], G V Kolmakov[1,3,4], L P Mezhov-Deglin[3] and P V E McClintock[1,5]

[1] Department of Physics, Lancaster University, Lancaster LA1 4YB, UK
[2] Laboratory for Elementary-Particle Physics, Cornell University, NY 14853-5001, USA
[3] Institute of Solid State Physics RAS, Chernogolovka, Moscow region 142432, Russia
[4] Department of Chemical and Petroleum Engineering, Pittsburgh University, Pittsburgh, PA 15261, USA
E-mail: a.ganshyn@lancaster.ac.uk, v.efimov@lancaster.ac.uk, p.v.e.mcclintock@lancaster.ac.uk, ang43@cornell.edu, mezhov@issp.ac.ru and gek11@pitt.edu

New Journal of Physics **12** (2010) 083047 (10pp)
Received 28 June 2010
Published 24 August 2010
Online at http://www.njp.org/
doi:10.1088/1367-2630/12/8/083047

Abstract. We report our experiments on the formation of second sound acoustic turbulence in superfluid ^{4}He. The initial growth in spectral amplitude follows power laws that steepen rapidly with increasing harmonic number n, corresponding to a propagating front in frequency space. The lower growth exponents agree well with analytic predictions and numerical modeling. The observed increase in the formation delay with n validates the concept of self-similarity in the growth of wave turbulence.

[5] Author to whom any correspondence should be addressed.

Contents

1. Introduction

Turbulence may be defined as a far-from-equilibrium state of a nonlinear physical system whose energy distribution extends over many degrees of freedom. It takes many different forms, of which vortex turbulence [1, 2] is probably the best known. A common feature lies in energy transfer between the scale or frequency at which energy from an external source is pumped into the system and a different scale or frequency at which it can be transformed to heat via dissipative processes. Turbulence in systems of waves is widespread in nature and technology. It can arise e.g. among phonons in solids [3], in optical fibers and nonlinear optical media [4], on vibrating plates [5]–[7] and the surfaces of ferrofluids [8, 9], in sound waves in oceanic waveguides [10], as magnetic turbulence in interstellar gases [11], in shock waves in the solar wind coupled to the Earth's magnetosphere [12], in surface waves on liquid hydrogen [13] and in second sound in superfluid helium [14, 15]. Typically, there is a cascade-like transfer of turbulent energy towards the high frequency domain [14, 16], which is where dissipation mainly occurs.

Of special interest is the application of the wave turbulence (WT) concept to the description of energy transfer in superfluid systems far from equilibrium, including disturbed superfluid ^{4}He [17], nonequilibrium exciton–polariton condensates in a cavity [18, 19] and atomic Bose–Einstein condensates in a trap [20]. It has been shown theoretically and numerically [21, 22] that the evolution of acoustic WT is of key importance in the late stages of condensate formation. Although the existing theory can in principle illuminate the nonequilibrium properties of superfluid systems, no experimental studies of turbulent evolution have previously been reported. The concept of self-similar formation of WT is widely accepted in theory [17, 21, 23, 24] but, to our knowledge, this prediction has not previously been checked experimentally.

In what follows, we report the results of an experiment to study the evolutionary processes that occur during the build-up towards steady-state WT in superfluid ^{4}He, following the initial application of a periodic driving force to excite second sound in a resonant cavity. It was established earlier that second sound (temperature–entropy waves) provides an ideal model system for laboratory studies of steady-state wave turbulent phenomena, in particular because the nonlinear wave interactions can readily be adjusted and controlled. Under steady-state nonequilibrium conditions, with continuous energy injection and dissipation [14, 15], acoustic turbulence is formed whose energy balance is highly nonlocal in K-space, and a direct flux of energy through the spectral scales is established. We now demonstrate that the formation of this turbulent state is self-similar and that, in its initial stages, it is described by power laws for

the amplitudes of the spectral harmonics. The evolution can be understood as a formation front propagating in frequency space towards the high frequency domain.

The velocity of a second sound traveling wave depends on its amplitude and, to a first approximation, can be written as

$$u_2 = u_{20}\,(1+\alpha\delta T)\,, \tag{1}$$

where δT is the wave amplitude, u_{20} is the velocity of a wave of infinitely small amplitude and α is the nonlinearity coefficient of second sound, which is determined by the relation [25]

$$\alpha = \frac{\partial}{\partial T}\ln\left(u_{20}^3\frac{C}{T}\right),$$

where C is the heat capacity per unit mass of liquid helium at constant pressure and T is the temperature.

The nonlinearity coefficient α may be either positive or negative, depending on the temperature and pressure [25]–[27]. Under saturated vapor pressure (SVP), in the region of roton second sound (i.e. at $T > 0.9\,\mathrm{K}$), the nonlinearity coefficient is positive ($\alpha > 0$) at temperatures $T < T_\alpha = 1.88\,\mathrm{K}$ (like the nonlinearity coefficient of conventional sound waves in ordinary media), but it is negative ($\alpha < 0$) in the range $T_\alpha < T < T_\lambda$. Here, $T_\lambda = 2.176\,\mathrm{K}$ is the temperature of the superfluid-to-normal (He II to He I) transition. At $T = T_\alpha$, the nonlinearity coefficient passes through zero. The ease with which α can be adjusted (by alteration of T), and the large values that it can take, make second sound in He II ideal as a test bed for the study of nonlinear wave interactions and associated phenomena, including WT.

The frequency of second sound depends on its wave vector k as [28]

$$\omega = u_{20}k\left[1+\lambda\xi^2k^2+\cdots\right], \tag{2}$$

where $\xi = \xi_0(1-T/T_\lambda)^{-2/3}$, $\xi_0 \sim 2$–$3\,\mathrm{A}$ and $\lambda \sim 1$. We emphasize that the dispersion of second sound is significant within the close vicinity of the superfluid transition (i.e. for $T_\lambda - T < 1\,\mu\mathrm{K}$), but is very weak in the temperature range $T < 2.1\,\mathrm{K}$ relevant to the present investigations. However, the presence of non-zero dispersion is of key importance in the formation of weak turbulence in He II. It is well established that if the dispersion is exactly equal to zero, $\partial u_{20}/\partial k = 0$, the main mechanism of energy transport through the frequency scales is quite different from turbulence and can be associated with shock wave creation [29]. When the dispersion is positive but small, $\partial u_{20}/\partial k > 0$ (e.g. in the case of second sound in He II, given by equation (2) where the leading nonlinear term is quadratic over the amplitude, see equation (1)), the wave turbulent state is formed in a narrow cone of $\mathbf{k}$-vectors around the direction of propagation of the wave with $\mathbf{k} = \mathbf{k}_{\mathrm{drive}}$ [16]. The relative phases of waves with $\mathbf{k}$-vectors almost collinear to $\mathbf{k}_{\mathrm{drive}}$ (i.e. within the cone) are random, and a standard kinetic equation for waves can be used to describe the cascade-like, turbulent propagation of energy in the wave system [16, 30]. However, the interaction of waves with non-collinear wave vectors is controlled by higher nonlinear terms and is relatively small. That is, wave turbulence in He II is nearly one-dimensional, provided that the dispersion given by equation (2) is weak, i.e. the temperature of the helium bath is not close to T_λ. The formation of the wave turbulent regime in He II manifests itself in, for example, fluctuations in the wave field at high frequencies and in the establishment of a near-Gaussian probability distribution function for second sound wave amplitudes, as was observed earlier [31].

In section 2, we describe briefly the experimental arrangements. The results obtained are presented in section 3. In section 4, we discuss the results, present a numerical theory and consider the broader implications of this work.

2. Experimental details

The experiments used the second sound resonator described previously [14, 32]: a thin film heater capped one end of a cylindrical quartz tube of length $\ell = 7$ cm and diameter $D = 15$ mm. The other end was capped by a superconducting bolometer, whose transition temperature could be adjusted by changing an external magnetic field. The He II inside the cell was held under its saturated vapor pressure at a temperature of $T = 2.08$ K, where $(T_\lambda - T)/T_\lambda = 0.041$. The temperature signal from the bolometer was recorded by a digital oscilloscope and then transferred to a computer for analysis. The quality of the resonator reached $Q \sim 3000$ at the higher resonance numbers ($N > 10$) but was less at lower resonances, behavior that is understandable in terms of losses due to normal fluid motion in the boundary layer next to the wall.

3. Experimental results

Figure 1(a) plots a typical evolution envelope following the step-like application of a resonant periodic drive to the heater under conditions such that there is no inverse energy cascade [15]. The standing wave in δT evolves nonmonotonically and often (as here) exhibits asymmetry. At early times, after switching on the drive, only a response at the driving frequency is evident, as shown by the power spectral density plotted in figure 1(b), corresponding to arrow-b in figure 1(a). Some time later, the direct energy cascade has become established in the low frequency domain, whereas the wave amplitude at high frequency remains close to zero, e.g. harmonics are formed only up to $\omega/2\pi < 20$ kHz in figure 1(c). At later times, the cascade is fully formed up to ~ 80 kHz, as shown in figure 1(d), corresponding to arrow-d in figure 1(a).

We now examine how the harmonics of the driving force evolve with time by analysis of the heights of the Fourier spikes labeled 1–5 in figure 1(d). The set of results plotted in figure 2 corresponds to the time domain signal shown in figure 1(a). It is immediately evident that each of the harmonic amplitudes grows initially according to a power law, undergoes shallow oscillations and finally flattens out as the steady state is approached. It is also clear that the corresponding power-law exponents at early times increase with the harmonic number n and that the higher harmonics develop after short delays.

4. Discussion and theory

To try to account for these phenomena, we apply the numerical model used earlier [14] for the computation of steady-state spectra. Energy balance is governed by

$$\mathrm{i}\frac{\partial b_n}{\partial t} = \sum_{n_1,n_2} V_{n,n_1,n_2}(b_{n_1}b_{n_2}\delta_{n-n_1-n_2} + 2b_{n_1}b^*_{n_2}\delta_{n_1-n_2-n}) - \mathrm{i}\gamma_n b_n + F_\mathrm{d}, \tag{3}$$

where $b_n(t) = (1/2)(B_n^{-1}S_n + \mathrm{i}B_n\beta_n)$ is the time-dependent canonical amplitude of second sound at the nth resonant frequency f_n; S_n and β_n are the space Fourier components

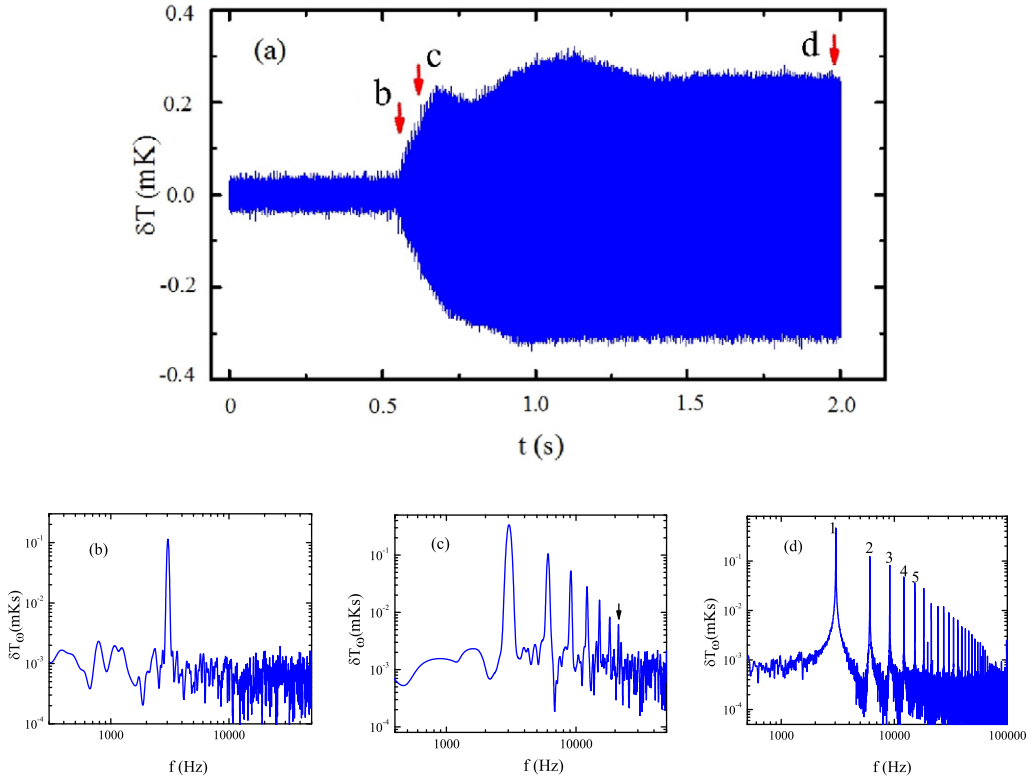

Figure 1. (a) Evolution with time t of the amplitude δT of the second sound standing wave at $T = 2.08\,\mathrm{K}$ after applying a resonant drive of amplitude 5.0 V to the heater at time $t = 0.55\,\mathrm{s}$. The ac flux from the heater was $W = 30\,\mathrm{mW\,cm^{-2}}$, and the generator frequency (half the second sound driving frequency) was $f/2 = 1523.23\,\mathrm{Hz}$, corresponding to the 31st resonance of the cavity. Individual periodic oscillations are not resolved in (a), which just shows their envelope; panels (b), (c) and (d) plot power spectra δT_ω computed within small windows at the positions shown by arrow-b, arrow-c and arrow-d in (a), respectively.

$\sim \cos(2\pi f_n x/u_{20}L)$ of the entropy and of the potential of the normal-superfluid relative velocity; $B_n = (f_n C/T)^{1/2}$; $V_{n,n_1,n_2} \propto \alpha(nn_1n_2)^{1/2}$ describes the three-wave interaction; $\gamma_n = \nu n^2$ models the viscous damping of second sound; and $F_\mathrm{d} \propto W$ is the amplitude of the force driving the nth resonant mode. In this representation, the wave spectrum can be calculated as $A_f \propto B_n\,(b_n + b_n^*)$.

To capture the dependence of the formation process on the driving force amplitude, we compute the evolution of the second sound wave spectrum with time for the driving force $F_\mathrm{d} = 1$ (in numerical units). The steady-state spectrum established at large times, i.e. after all transient processes are finished at $t_\mathrm{form} \geqslant 5$, is shown in figures 3(a) by circles. Figure 3(a) also demonstrates the evolution of the spectrum during the build-up process, similar to that observed in the experiments (figures 1(b)–(d)).

Figure 3(b) shows the dependence on time of the amplitude of the wave at the driving frequency and of two higher harmonics computed for the evolution presented in figure 3(a). It

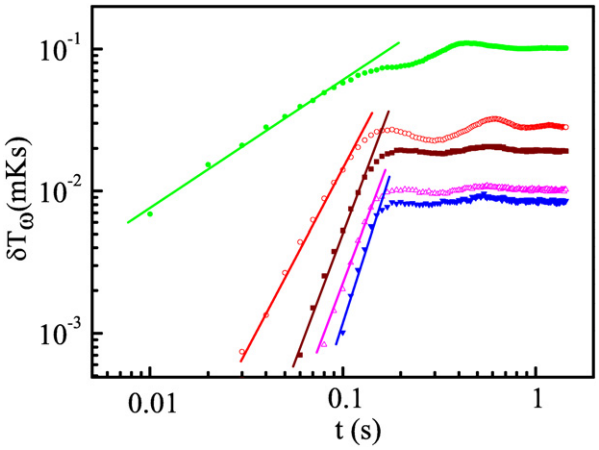

Figure 2. Evolution with time t of the first five harmonics in the time domain signal shown in figure 1(a), plotted on log–log scales. The sets of points correspond to $n = 1, 2, \ldots, 5$, from the top to bottom, respectively, with gradients for linear fits of 1.0 ± 0.3, 2.7 ± 0.3, 4.3 ± 0.5, 4.7 ± 0.5 and 6.0 ± 0.5.

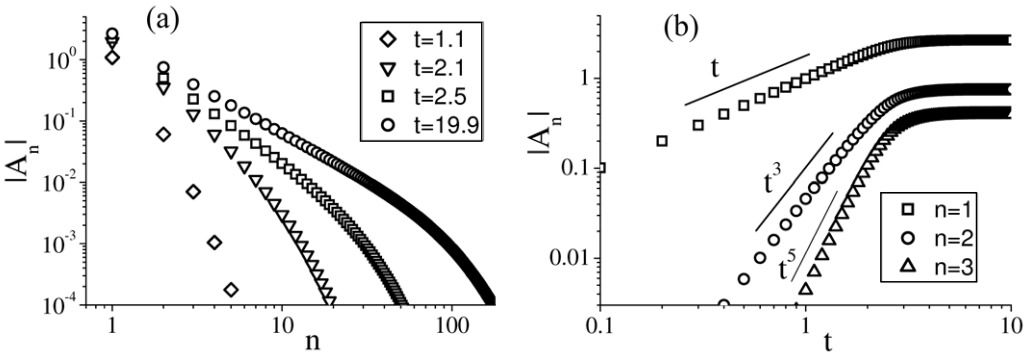

Figure 3. Results from the numerical model. Note the log–log scales. (a) Evolution with time t of the spectral amplitude during the build-up of turbulence. (b) Points: dependences on t of the spectral amplitude at driving frequency, $|A_1|$, and of higher harmonics, $|A_n|$, with $n > 1$. Lines: dependences $|A_n| \propto t^{2n-1}$. The computations were for $F_\mathrm{d} = 1$.

is evident that the dependences of the wave amplitudes on time during the formation process $t < 2$ are well described by a power-law function,

$$|A_n| \propto t^m, \tag{4}$$

where $m = 2n - 1$. We see also that the characteristic formation time is $t_\mathrm{form} \sim 5$.

We can account for the observed dependence (4) analytically within the framework of the model (3). It is evident from figure 3(b) that, at small times $t \ll t_\mathrm{form}$, the wave amplitude is also small. During this era, it is the wave at the driving frequency that has the largest amplitude. We may therefore reduce the whole set of equation (3) to a simpler form $\mathrm{d}A_1/\mathrm{d}t = F_\mathrm{d}$, $\mathrm{d}A_n/\mathrm{d}t = V_{n,1,n-1}A_1A_{n-1}$ $(n > 1)$. We neglect dissipation, which has a negligible effect early in

the growth process. The reduced equations imply that the wave at the driving frequency, $n = 1$, grows mainly due to interaction with the driving force, and the evolution of each $n > 1$ harmonic is defined by the interaction with its left-hand side neighbor, A_{n-1}, and with the fundamental wave, A_1. From the reduced equations, one finds $A_1 = F_\mathrm{d} \times t$ for $n = 1$ and $A_n = \tilde{V}_n F_\mathrm{d}^n t^{(2n-1)}$, where $\tilde{V}_n = (1/(2n-1)!!)\Pi_{k=2}^n V_{k,1,k-1}$ for $n > 1$ and !! signifies a double-factorial. The result obtained clearly agrees well with the numerical computations (figures 3(b) and equation (4)). The exponents $m = 2n - 1$ are *universal* and do not depend on the value of the nonlinearity coefficient (at $V_{k,l,m} \propto \alpha \neq 0$) or on the driving amplitude F_d. The model is valid for small $t \ll t_\mathrm{form}$.

The results from the numerical model compare well with those from the experiments. In both cases, the initial growth in spectral amplitude takes the form of a power law whose exponent grows with increasing harmonic number n. For $n = 1, 2$, the measured exponents agree within experimental error with the values of 1 and 3 predicted by equation (4). For larger n, the experimental exponents still increase with n, but the agreement becomes only qualitative. We comment, however, that such discrepancies are to be expected, because at larger times when the low-frequency harmonics are not small with respect to their equilibrium values, nonlinear interactions other than those taken into account in the reduced equations start playing an essential role.

To analyze the details of the turbulence build-up process at larger t, we suppose that formation is self-similar with a finite formation time t^* (i.e. of the explosion type for WT [16], corresponding to the case of a finite capacity spectrum [33]). In agreement with general recommendations [16, 17, 33], in this case the harmonic amplitude at frequency ω, time t, can be estimated as $A(\omega, t) = (t^* - t)^q f(\xi)$, where $\xi = \omega(t^* - t)^p$ is the self-similar variable, f is a universal function that describes the evolution of the wave spectrum in the course of the build-up process, and q and p are positive exponents. The f function obeys the boundary conditions [16] $f \propto \xi^{-s}$ at $\xi \ll 1$ and $f\xi^s \to 0$ at $\xi \gg 1$, where $s \approx 1$ is close to the Kolmogorov index of the steady-state turbulent spectrum taken with opposite sign [14, 33]. (The indices also satisfy the relation $q = sp$, to ensure the steady-state character of the spectrum formed for $\xi \ll 1$; see below.) According to the boundary conditions, in the low frequency domain $\xi \ll 1$, a spectrum $A_\omega \propto \omega^{-s}$ is formed, and in the high frequency domain $\xi \gg 1$, the harmonic amplitudes are close to zero. At the characteristic transition frequency between the two domains, ω_f, one has $\xi \sim 1$ [17]. As a result, the transient process can be understood as the propagation of a formation front in frequency space from low to high frequencies, whose position at time t is

$$\omega_\mathrm{f} = \mathrm{const} \times (t^* - t)^{-p}. \tag{5}$$

This conclusion agrees with the experimental observations shown in figure 1 and in the numerical simulations of figure 3(a). For example, the position of the front at $t = 0.66\,\mathrm{s}$ is marked by an arrow in figure 1(c). (Note that under experimental conditions the cascade is restricted at a high frequency ω_b due to viscosity [14], hence the dependence (5) is only valid at $\omega_\mathrm{f} < \omega_b$.)

To capture the details of the front propagation, we plot in figure 4 the characteristic delay time of harmonic formation as a function of n for the first 12 harmonics. The formation delay Δt_n is defined as the interval between the application of the driving force at t_on and the time t_n when the nth harmonic rises from the common noise floor. The formation delay of the fundamental wave, $n = 1$, is negligible. The steady growth of t_n with n in figure 4 corresponds to the finite propagation velocity of the front, $\mathrm{d}\omega_\mathrm{f}(t)/\mathrm{d}t$, in agreement with equation (5). It

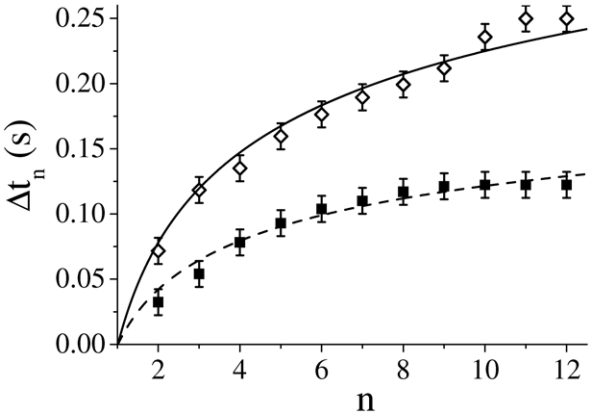

Figure 4. Experimental formation delays Δt_n for the 31st resonance with $W = 30.0\,\mathrm{mW\,cm^{-2}}$ (filled squares) and for the 15th resonance with $W = 58.8\,\mathrm{mW\,cm^{-2}}$ (open lozenges). The dashed and full curves are least-squares fits of equation (6) with $C = 0.331$ and 0.613 s, respectively, for $p = 5.0$.

follows from (5) that the difference between the formation times of the nth and 1st harmonics is equal to $t_n - t_1 = \mathrm{const} \times (\omega_1^{-1/p} - \omega_n^{-1/p})$. Noting that the frequency of the nth harmonic is $\omega_n = n \times \omega_1$, one obtains

$$\Delta t_n = t_n - t_{\mathrm{on}} = C \times (1 - n^{-1/p}), \tag{6}$$

where C is a constant of the order of t_{form}. The experimental points in figure 4 can be closely fitted by (6) (curves) for $p = 5.0$. Thus the experimental data are well described by the self-similar dependence (6).

5. Conclusions

We have reported the first experimental study of the processes involved in the creation of steady-state acoustic turbulence in a superfluid system. In the main, the results are well described by a numerical model, although there are points of detail that are not captured. These include the damped oscillations seen in the spectral amplitudes as the steady state is approached, and discrepancies in the measured and calculated power-law exponents describing the initial growth for $n \geqslant 3$. Up to intermediate times, the build-up of turbulence is well described by the self-similar model (5). These same considerations should also be applicable to the other systems described in the Introduction for which, however, the experimental conditions and parameters are in many cases much harder to control.

Acknowledgments

We are grateful for valuable discussions with E A Kuznetsov, V Lebedev and A A Levchenko. This work was supported by the Engineering and Physical Sciences Research Council (UK), by the Russian Foundation for Basic Research, by the Presidium of the Russian Academy of Sciences under the program 'Fundamental Problems of Nonlinear Dynamics' and by the Royal Society of London.

References

[1] Tritton D J 1988 *Physical Fluid Dynamics* 2nd edn (Oxford: Clarendon)

[2] Davidson P A 2004 *Turbulence: An Introduction for Scientists and Engineers* (Oxford: Oxford University Press)

[3] Tsoi V S 2003 Transverse electron focusing as a way of studying phonon kinetics turbulence of phonon flow *Central Eur. J. Phys.* **1** 72–90

[4] Bortolozzo U, Laurie J, Nazarenko S and Residori S 2009 Optical wave turbulence and the condensation of light *J. Opt. Soc. Am.* B **26** 2280–4

[5] Boudaoud A, Cadot O, Odille B and Touze C 2008 Observation of wave turbulence in vibrating plates *Phys. Rev. Lett.* **100** 234504

[6] Mordant N 2008 Are there waves in elastic wave turbulence? *Phys. Rev. Lett.* **100** 234505

[7] Cobelli P, Petitjeans P, Maurel A, Pagneux V and Mordant N 2009 Space-time resolved wave turbulence in a vibrating plate *Phys. Rev. Lett.* **103** 204301

[8] Boyer F and Falcon E 2008 Wave turbulence on the surface of a ferrofluid in a magnetic field *Phys. Rev. Lett.* **101** 244502

[9] Falcon E 2010 Laboratory experiments on wave turbulence *Discrete Cont. Dyn. Syst.* B **13** 819–40

[10] Gurbatov S N, Kurin V V, Kustov L M and Pronchatov-Rubtsov N V 2005 Physical modeling of nonlinear sound wave propagation in oceanic waveguides of variable depth *Acoust. Phys.* **51** 152–9

[11] Bisnovatyi-Kogan G S and Silich S A 1995 Shock-wave propagation in the nonuniform interstellar medium *Rev. Mod. Phys.* **67** 661–712

[12] Ryutova M and Tarbell T 2003 MHD shocks and the origin of the solar transition region *Phys. Rev. Lett.* **90** 191101

[13] Kolmakov G V, Levchenko A A, Brazhnikov M Yu, Mezhov-Deglin L P, Silchenko A N and McClintock P V E 2004 Quasi-adiabatic decay of capillary turbulence on the charged surface of liquid hydrogen *Phys. Rev. Lett.* **93** 074501

[14] Kolmakov G V, Efimov V B, Ganshin A N, McClintock P V E and Mezhov-Deglin L P 2006 Formation of a direct Kolmogorov-like cascade of second sound waves in He II *Phys. Rev. Lett.* **97** 155301

[15] Ganshin A N, Efimov V B, Kolmakov G V, Mezhov-Deglin L P and McClintock P V E 2008 Observation of an inverse energy cascade in developed acoustic turbulence in superfluid helium *Phys. Rev. Lett.* **101** 065303

[16] Zakharov V E, L'vov V S and Falkovich G 1992 *Kolmogorov Spectra of Turbulence I* (Berlin: Springer)

[17] Kolmakov G V 1995 Acoustic turbulence in media with two types of sound *Physica* D **86** 470–9

[18] Kasprzak J *et al* 2006 Bose–Einstein condensation of exciton polaritons *Nature* **443** 409–14

[19] Amo A *et al* 2009 Collective fluid dynamics of a polariton condensate in a semiconductor microcavity *Nature* **457** 291–3

[20] Griffin A, Nikuni T and Zaremba E 2009 *Bose-Condensed Gases at Finite Temperatures* (New York: Cambridge University Press)

[21] Zakharov V E and Nazarenko S V 2005 Dynamics of the Bose–Einstein condensation *Physica* D **201** 203–11

[22] Nazarenko S and Onorato M 2006 Wave turbulence and vortices in Bose–Einstein condensation *Physica* D **219** 1–12

[23] Falkovich G E and Shafarenko A V 1995 Nonstationary wave turbulence *J. Nonlinear Sci.* **1** 457–80

[24] Connaughton C, Newell A C and Pomeau Y 2003 Non-stationary spectra of local wave turbulence *Physica* D **184** 64–85

[25] Khalatnikov I M 1965 *An Introduction to the Theory of Superfluidity* (New York: Benjamin)

[26] Dessler A J and Fairbank W H 1956 Amplitude dependence of the velocity of second sound *Phys. Rev.* **104** 6–12

[27] Efimov V B, Kolmakov G V, Lebedeva E V, Mezhov-Deglin L P and Trusov A B 2000 Generation of second and first sound waves by a pulse heater in He-II under pressure *J. Low Temp. Phys.* **119** 309–22

[28] Tyson J A and Douglass D H Jr 1968 Critical-region second-sound velocity in He II *Phys. Rev. Lett.* **21** 1308–10
[29] Kadomtsev B B and Petviashvili V I 1970 On the stability of solitary waves in weakly dispersive media *Sov. Phys.—Dokl.* **15** 539–41
[30] Zakharov V E and Sagdeev R Z 1970 Spectrum of acoustic turbulence *Sov. Phys.—Dokl.* **15** 439–41
[31] Efimov V B, Ganshin A N and McClintock P V E 2008 Statistical properties of strongly nonlinear waves within a resonator *Phys. Rev.* E **78** 066611
[32] Efimov V B, Ganshin A N, McClintock P V E, Kolmakov G V and Mezhov-Deglin L P 2006 Experimental study of the nonlinear second sound wave interaction in superfluid ^{4}He *J. Low Temp. Phys.* **145** 155–64
[33] Connaughton C and Newell A C 2010 Dynamical scaling and the finite-capacity anomaly in three-wave turbulence *Phys. Rev.* E **81** 036303